Acta Pharmacologica Sinica (2009) 30: 1262–1275
 1671-4083/09 $32.00
www.nature.com/aps

Original Article

Molecular mechanisms underlying the cholesterol-lowering effect of *Ginkgo biloba* extract in hepatocytes: a comparative study with lovastatin

Zuo-quan XIE[1, 2], Gai LIANG[3], Lu ZHANG[1, 2], Qi WANG[2], Yi QU[2], Yang GAO[2], Li-bo LIN[2], Sai YE[2], Ji ZHANG[1], Hui WANG[3], Guo-ping ZHAO[2, 4], Qing-hua ZHANG[1, 2, 4, *]

[1]State Key Laboratory of Medical Genomics and Shanghai Institute of Hematology, Ruijin Hospital, Shanghai Jiaotong University School of Medicine, Shanghai 200025, China; [2]National Engineering Center for Biochip at Shanghai and Shanghai Biochip Co ltd, Shanghai 201203, China; [3]Department of Pharmacology, Basic Medical School of Wuhan University, Wuhan 430071, China; [4]Shanghai-MOST Key Laboratory of Health and Disease Genomics, Shanghai 201203, China

Aim: To explore the molecular mechanisms underlying the cholesterol-lowering effect of a *Ginkgo biloba* extract (GBE).
Methods: Enzyme activity, cholesterol flux and changes in gene expression levels were assessed in cultured hepatocytes treated with GBE or lovastatin.
Results: GBE decreased the total cholesterol content in cultured hepatocytes and inhibited the activity of HMG-CoA reductase, as determined by an *in vitro* enzyme activity assay. In addition, GBE decreased cholesterol influx, whereas lovastatin increased cholesterol influx. GBE treatment induced significant increases in the expression of cholesterogenic genes and genes involved in cholesterol metabolism, such as *SREBF2*, as determined by cDNA microarray and real-time RT-PCR. Furthermore, *INSIG2*, *LDLR*, *LRP1*, and *LRP10* were differentially regulated by GBE and lovastatin. The data imply that the two compounds modulate cholesterol metabolism through distinct mechanisms.
Conclusion: By using a gene expression profiling approach, we were able to broaden the understanding of the molecular mechanisms by which GBE lowers cellular cholesterol levels. Specifically, we demonstrated that GBE exhibited dual effects on the cellular cholesterol pool by modulating both HMG-CoA reductase activity and inhibiting cholesterol influx.

Keywords: *Ginkgo biloba* extract; cholesterol; HMG-CoA reductase; influx; lovastatin; microarray

Acta Pharmacologica Sinica (2009) 30: 1262–1275; doi: 10.1038/aps.2009.126; published online 24 August 2009

Introduction

Ginkgo biloba extract (GBE) is being increasingly used as a dietary supplement for the treatment of a variety of neurological and cardiovascular disorders. The main active components of the standard GBE are flavonol glycosides (~24% total volume) and terpene lactones (~6%)[1]. The mixture of biologically active ingredients present in GBE has pleiotropic physiological effects, including the inhibition of amyloid-formation[2, 3], antioxidant activity[4, 5], anti-apoptosis activity[6], effects on vasodilation[7] and inhibition of platelet aggregation[8, 9]. Recently, studies have shown that GBE modulates the metabolism of cholesterol. GBE decreased the blood cholesterol level in rats and rabbits fed a cholesterol-enriched diet[10–12]. In humans, GBE ingestion reduces the formation and size of atherosclerotic nanoplaques in high-risk cardiovascular patients and attenuates risk factors, including oxidized low-density lipoprotein (oxLDL)/low density lipoprotein (LDL) and lipoprotein Lp(a)[13]. These observations reveal the modulating effect of GBE on cholesterol metabolism; however, the underlying mechanisms remain undefined.

The liver is the major source of endogenous cholesterol biosynthesis and is largely responsible for the maintenance of blood cholesterol homeostasis. Therefore, we used two cultured human hepatocellular carcinoma cell lines, HepG2, and SK-HEP-1, in the present study to evaluate the cholesterol-lowering effect of GBE. In addition, we used lovastatin, a well-known cholesterol-lowering medication, as our positive control. To investigate the mechanisms underlying the

The original microarray data have been submitted to GEO (accession number GSE11830).
* To whom correspondence should be addressed.
E-mail qinghua_zhang@shbiochip.com
Received 2008-12-29 Accepted 2009-03-09

cholesterol-lowering effect of GBE, we used a combination of experimental approaches, including enzyme activity and cholesterol flux assays, along with cDNA microarray and real time RT-PCR, to explore the gene regulation networks that are downstream of GBE treatment. Data presented here bring a new understanding to the molecular mechanisms by which GBE affects cholesterol metabolism.

Materials and methods

Cell culture and treatment

GBE was provided by XingLing Pharmaceutical Co (Shanghai, China) as a standardized product that contains ~24% flavonol glycosides, ~6% terpene lactones (ginkgolides, bilobalide), and less than ~5 ppm ginkgolic acid. HepG2 cells were maintained in Minimum Essential Medium (MEM, Invitrogen) with 10% fetal bovine serum (FBS) (JRH Biosciences). Cells were seeded in 6-well plates at a density of 4×10^5 cells per well. When the cells were about 70% confluent, the medium was replaced with medium containing 2% FBS for drug treatment experiments. For dose-response experiments, a variety of concentrations of GBE (50, 100, and 200 μg/mL) were used, and the cells were treated for 24 h. For time course experiments, cells were treated for different times (6, 12, 24, and 48 h) with either 200 μg/mL of GBE or 0.5 μmol/L lovastatin. Control cells were treated with 0.1% DMSO (the vehicle) for the longest treatment time in the experiment. Treatments were identical for both the SK-HEP-1 and the HepG2 cell lines, with the exception that SK-HEP-1 cells were cultured in Dulbecco's modified Eagle's medium (DMEM, Invitrogen).

Cellular cholesterol measurement

Cellular total cholesterol was extracted as previously reported[14] with slight modifications. Briefly, cells were harvested and washed twice with PBS, followed by resuspension in 1 mL isopropanol and sonication for 20 min at 4 °C. After centrifugation at 9000 ×*g* for 10 min at 4 °C, the supernatant was evaporated under a vacuum and the pellet was resuspended in 20 μL isopropanol for cellular cholesterol measurement. The cholesterol was measured colorimetrically using a Total Cholesterol Detection Kit (Jiemen Bio-Tech, Shanghai, China). Additionally, the sediment fractions were lysed using a Mammalian Cell Extraction Kit (BioVision). Total protein levels were quantified by the Bradford method.

HMG-CoA reductase enzymatic activity assay

The activity of HMG-CoA reductase was measured according to a previously published method[15] with slight modifications. Briefly, microsomes were prepared from the livers of rats. The assay was performed in a total volume of 120 μL containing 500 nmol NADPH (dissolved in 0.1 mol/L triethanolamine and 10 mmol/L EDTA) and 100 μg of microsomes. After a 5 min preincubation at 37 °C, 5.17 nmol [^{14}C]HMG-CoA (GE Healthcare), with or without GBE or lovastatin, was added to the system (final concentration 38.3 μmol/L and 2.14 GBq/mmol, respectively). After a 15 min incubation at 37 °C, the reaction was terminated by the addition of 30 μL of 6 mol/L HCl. The samples were incubated for 15 min at 37 °C to allow complete lactonization of the mevalonic acid, followed by centrifugation at 9000×*g* for 10 min. The supernatants were spotted onto silica gel GF254 TLC plates, and the chromatograms were developed in benzene-acetone 1:l (*v/v*). [^{14}C]MVA lactone (GE Healthcare) was used as a reference. The [^{14}C] radioactivity was determined with a liquid scintillation counter (LS6500, Beckman-Coulter). HMG-CoA reductase activity was calculated as μmol of mevalonate generated per minute per mg of microsomes at 37 °C.

Cholesterol influx and efflux assay

Cholesterol influx and efflux assays were carried out according to the methods described by Yao *et al*[10]. For the cholesterol influx measurements, 2×10^5 HepG2 cells were seeded in 24-well plates and cultured in MEM plus 10% FBS. When the cells reached 75%−80% confluence, the medium was replaced with 0.5 mL MEM containing 2% FBS and 0.2 μCi [1α,2α(n)-^{3}H] cholesterol (GE Healthcare) and the presence or absence of either various concentrations of GBE (50, 100, and 200 μg/mL) or lovastatin (0.5 μmol/L). After 24 h of treatment, the cells were washed with PBS twice and lysed in 200 μL of 0.1 mol/L NaOH. Radioactivity was measured by a liquid scintillation counter (LS6500, Beckman-Coulter). Protein levels were quantified by the Bradford method.

For the efflux assay, 2×10^5 HepG2 cells were seeded in 24-well plates and cultured with MEM plus 10% FBS and 0.2 μCi [1α,2α(n)-^{3}H]cholesterol in each well for 48 h. After incubation, the cells were washed twice with MEM plus 10% FBS and FBS-free medium. Then, the cells were treated with the indicated concentrations of GBE and lovastatin in 0.5 mL MEM plus 2% FBS for 24 h. A volume of 200 μL of medium was used to determine the level of radioactivity. Protein levels were quantified as described above.

cDNA microarray

After the time course experiments, cells were collected and total RNA was extracted using TRIzol reagent (Invitrogen), followed by purification on an RNeasy column (Qiagen) and quantified by UV absorption (Nanodrop). RNA quality was assessed with a 2100 Bioanalyzer and the RNA 6000 LabChipR (Agilent Technologies). The SBC homemade human cDNA microarray (Shanghai, China) contains 15552 spots, including 768 controls and 14784 probes. The probes represent 10379 known genes and 3022 ESTs. The microarray was made as previously described[16]. An Agilent Low RNA Input Fluorescent Linear Amplification Kit (Agilent Technologies) was used for RNA linear amplification following the manufacturer's protocol. RNA samples from three wells of the vehicle treated group were pooled and used as a reference to label Cy3 (GE Healthcare). RNA from the drug treated cells was isolated in triplicate and labeled with Cy5 individually. Cy3- and Cy5-labeled cRNA pools were mixed to hybridize to the microarrays. Hybridization and washes were performed using a standard protocol, followed by scanning on a Axon 4000B Scanner (Axon Instruments)[17].

Data analysis

Data analysis between and within the chip's normalization was performed by locally weighted scatter plot smoothing (LOWESS) regression[18]. Only genes present in greater than 80% of the samples were filtered out for further analysis. A total of 9510 genes/ESTs were selected out. The log2 ratio of each gene/EST is available at the following Web site: www.shbiochip.com/research/GBE/HepG2. Principal Components Analysis (PCA) was applied to distinguish between different groups. Gene expression profiling at each time point was analyzed with Significance Analysis of Microarray software (SAM, version 2.20)[19] with One Class response type (FDR<0.01). Differentially expressed genes were chosen if they fit at least one of the following criteria: 1) genes were regulated in at least one time point by either GBE or lovastatin, 2) genes were differentially expressed between GBE and lovastatin treatment in at least one time point, or 3) gene expression levels were different among the different time points for either GBE or lovastatin. A total of 1264 regulated genes/ESTs were selected out and presented using a component plane presentation integrated self-organizing map (CPP-SOM)[20] with 12 neurons based on the gene expression profile. The online database KEGG (www.genome.jp/kegg) was applied to interpret the gene function pathway.

Real-time RT-PCR

Total RNA from each sample used for the microarray experiment was subjected to reverse transcription. Real-time RT-PCR was conducted using an ABI PRISM 7300 Sequence Detector (Applied Biosystems) with SYBR green I fluorescent dye (Toyobo, Japan). The reactions were carried out in triplicate. *GAPDH* was used as an internal control. Gene expression was evaluated with threshold cycles. The gene names and PCR primer sequences are listed in Table S1.

Western blot analysis

Proteins were prepared with the Mammalian Cell Extraction Kit (BioVision). An aliquot of each sample (50 μg) was subjected to SDS-polyacrylamide (10%) gel electrophoresis and electro-transferred onto a PVDF membrane. After being blocked with 5% nonfat milk, the membranes were individually probed with the following primary antibodies for 2 h:

Table S1. Primer sequences of the genes subjected to real-time RT-PCR.

Symbol	Genebank	Forward primer	Reverse primer	Microarray covering	Array detect
ABCA1	NM_005502	AAGCTCTTTGCACTAGGATGGC	TGTAGCATGTTCCGGTGTTTCTC	P	ND
ABCG5	NM_022436	GACTGCTCTGAACGTCTGAAATG	TTTCCAAATAACCACATGTCCC	NA	
ABCG8	NM_022437	TCCTGCGGTGGTGTTTTG	CGATGAGGTAGATGGCGTA	NA	
APOA1	NM_000039	ACCTAAAGCTCCTTGACAAC	CCTGCCACTTCTTCTGGA	P	R
APOB	NM_000384	AAGAACCTGTTAGTTGCTCTTAAGG	TTCTTCGTCGCAATGGCCT	NA	
CYP7A1	NM_000780	GGATGTATTCTTTCTGCTACCGAG	CGCAGTCCTGAACATGTGAA	NA	
DAF	NM_000574	TTTAAAATGGTCCACAGCAGTC	ATAATATGCCACCTGGTACATC	NA	
DHCR7	NM_001360	AGTCACCTTTACTAGTCCTTTGG	GTAAATGCAGCCTAATGACAG	P	R
ELOVL6	NM_024090	TGCACTGGTATCACCACATCAC	TGCACGCCATAGTTCATAGTCA	P	R
NR1H4	NM_005123	TTTTGACGGAAATGGCAACC	TCAGAATGCCCAGACGGAAG	P	
GAPDH	NM_002046	TGACTTCAACAGCGACACCCA	CACCCTGTTGCTGTAGCCAAA	P	IC
HMGCR	NM_000859	TAGGAGGCTACAACGCCCAT	CCACCCACCGTTCCTATCTC	P	R
IDI1	NM_004508	GGCTGAAAGCTGAGCTAGGA	TTTCATGTTCACCCCAGATAC	P	R
IGFBP1	NM_000596	TGCCAAACTGCAACAAGAATG	TGGAGACCCAGGGATCCT	P	R
INSIG2	NM_016133	AATGGCAACCAGCACCTC	CATGCACAGACACATTCTCTC	NA	
KIAA0101	NM_014736	AACTCCCAAGTGGCAAAAAGG	TGTGTGATCAGGTTGCAAAGG	P	R
LDLR	NM_000527	GATTCATGTGGCAAGAACG	AGCTGAACTCACCGGATCG	P	ND
LRH1	NM_205860	TCGCCGATCAGAGCTCATA	CATTCCTCTCCATGTATCTTCTA	NA	
LRP1	NM_002332	GCCTCCATCCTAATCCCTCT	GGTTTCCAATCTCCACGTTCA	P	ND
LXRA	NM_005693	GACTTTGCTAAACAGCTACCC	CTGCTTTGGCAAAGTCTTC	P	ND
MTTP	NM_000253	TATATGCAGTATGCTACCCACAGC	GTACCAAATGAGATTTGAGAGAGGT	P	ND
NPC1L1	NM_013389	CATCTCTATGGGAAGTGCGGT	CCACGTAGCTGAGGATGAC	P	ND
PCNA	NM_002592	ATAAAGAGGAGGAAGCTGTTAC	AGAGAGTGGAGTGGCTTTTG	P	R
SCAP	NM_012235	CCAGTGGAGGACAAGATGGG	CAGGTAAGGGAGGTGACAT	NA	
SCARB1	NM_005505	CATGAAATCTGTCGCAGGC	TTTGGCAGATGACAGGGAC	NA	
SHP	NM_021969	TGCCTGAAAGGGACCATC	ACTTCACACAGCACCCAGT	P	ND
SLC35B1	NM_005827	GGGTCTTGGTCTTGATGCC	CCAAGAGATGTCACTGTTTGA	P	R
SOAT1	NM_003101	GACTTGTCGTTACGTGTTTTAG	CAGTTTGGCTTCAAGTGAC	P	ND
SREBF2	NM_004599	TCACTCCCTGGGAAAGC	CAGTAGCAGGTCACAGGT	P	ND

microarray covering: P, presented in the genelist of the microarray; NA, not included in the genelist of the microarray; array detect: R, regulation detected with microarray, ND, no regulation detected with microarray; IC, internal control used; blank, not presented in the microarray

β-actin (1:5000, Abcam), HMGCR (1:800, sc-27578, Santa Cruz Biotechnologies), SREBP2 N-terminus (1:200, sc-8151, Santa Cruz Biotechnologies), and SREBP2 C-terminus (1:200, sc-13552, Santa Cruz Biotechnologies). Then, the membranes were incubated with a horseradish peroxidase (HRP) conjugated secondary antibody, either goat anti-mouse (1:4000, Sigma) or donkey anti-goat (1:800, homemade). The membranes were visualized with ECL Plus reagent (GE Healthcare) and developed onto X-ray film (Kodak).

Results

Cholesterol lowering effect of GBE in hepatocytes

To determine whether GBE modulates cholesterol levels in hepatocytes, HepG2, and SK-HEP-1 cells were cultured in medium with or without various concentrations of either GBE or lovastatin (positive control). The total cholesterol content was measured using a colorimetric assay. After 24 h of treatment, GBE decreased the total cholesterol content in a dose-dependent manner in both HepG2 and SK-HEP-1 cells. Lovastatin (0.5 μmol/L) also decreased the total cholesterol content (Figure 1A, 1B). In HepG2 cells, both 0.5 μmol/L of lovastatin and 200 μg/mL of GBE demonstrated a time-dependent effect on cholesterol content. The maximum cholesterol reduction was observed at 24 h, whereas a moderate recovery was observed after 48 h (Figure 1C, 1D).

Inhibition of HMG-CoA reductase activity

To test whether GBE affects the activity of HMG-CoA reductase, the rate limiting enzyme in cholesterol biosynthesis, we performed an experiment using *in vitro* reacted hepatic microsomes. The activity of HMG-CoA reductase was inhibited by both GBE and lovastatin. A dose of 129 nmol/L of lovastatin inhibited the HMG-CoA reductase activity by 25.2%. GBE inhibited HMG-CoA reductase activity by 6.2%, 16% and 71.6% at concentrations of 32.26, 322.6, and 3226 μg/mL, respectively (Table 1).

Table 1. Effect of GBE and lovastatin on HMG-CoA reductase activity in *in vitro* experiment. n=3 for each group. Mean±SD. $^bP<0.05$, $^cP<0.01$ *vs* control group using One-Way ANOVA.

Group	Concentration	Activity (10^{-5} μmol·min^{-1}·mg^{-1})	Inhibition (%)
Control	0	55±0.7	0
GBE	32.26 μg/mL	52±1.8^b	6.2±2.5
	322.6 μg/mL	47±1.6^c	16.0±2.5
	3226 μg/mL	16±4.1^c	71.6±7.1
Lovastatin	129 nmol/L	40±3.6^c	27.2±6.8

Effect of GBE on cholesterol fluxes in HepG2 cells

We determined the effect of GBE on cholesterol flux. In HepG2 cells, lovastatin induced a significant increase in cholesterol influx. In contrast, GBE inhibited cholesterol influx in a dose-dependent manner (Figure 2A). No significant alterations in cholesterol efflux were observed in HepG2 cells treated with either GBE or lovastatin (Figure 2B).

Transcriptomic profiling induced by GBE in HepG2 cells

To determine the mechanisms underlying the effect of GBE on cholesterol lowering, we performed microarray analysis. The global transcriptomic profiling of the cells treated with either GBE or lovastatin is shown with PCA plots. We identified 1264 regulated genes/ESTs, which are shown as PCA and CPP-SOM (Figure 3A, 3B, www.shbiochip.com/research/GBE/HepG2). These results demonstrate a similar gene expression profile regulation of both GBE and lovastatin. With ontology annotations, 254 of the regulated genes were

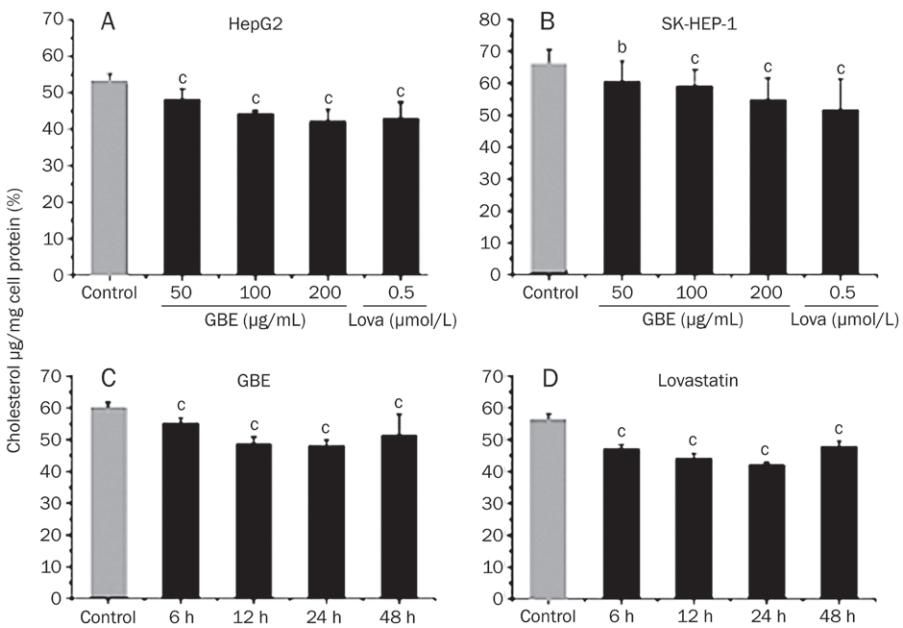

Figure 1. GBE and lovastatin decreased the total cholesterol content in cultured hepatocytes. (A, B) HepG2 and SK-HEP-1 cells were treated with GBE (50, 100, 200 μg/mL) or lovastatin (0.5 μmol/L) for 24 h in MEM-2%FBS media, and the total cholesterol content was decreased in a dose-dependent manner. (C, D) GBE (200 μg/mL) and lovastatin (0.5 μmol/L) decreased the cellular total cholesterol content in a time-dependent manner (6, 12, 24 h) in MEM-2%FBS media, while a moderate recovery was observed after 48 h of treatment. n=3 independent experiments. Mean±SD. $^bP<0.05$, $^cP<0.01$ *vs* control group using One-way ANOVA.

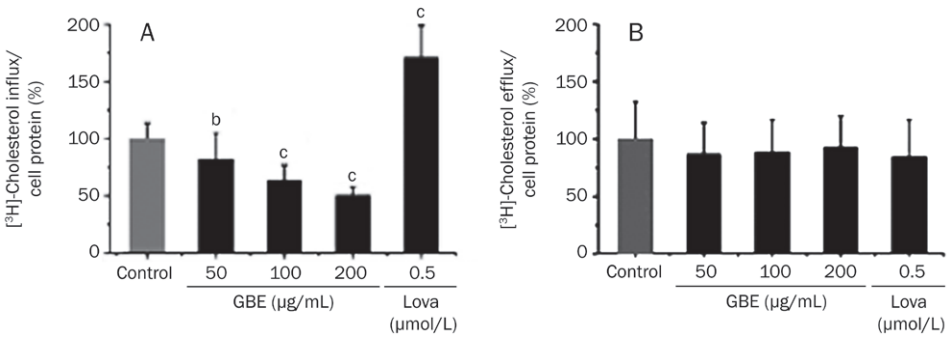

Figure 2. Effect of GBE and lovastatin on cholesterol fluxes in HepG2 cells. (A) Cholesterol influx was inhibited by GBE in a dose-dependent (50, 100, and 200 μg/mL) manner in MEM-2%FBS after 24 h of treatment, whereas it was increased by lovastatin. (B) Cholesterol efflux was not significantly altered by GBE or lovastatin in MEM-2%FBS after 24 h of treatment. Mean±SD from three independent experiments. $^{b}P<0.05$, $^{c}P<0.01$ *vs* the control group using One-Way ANOVA.

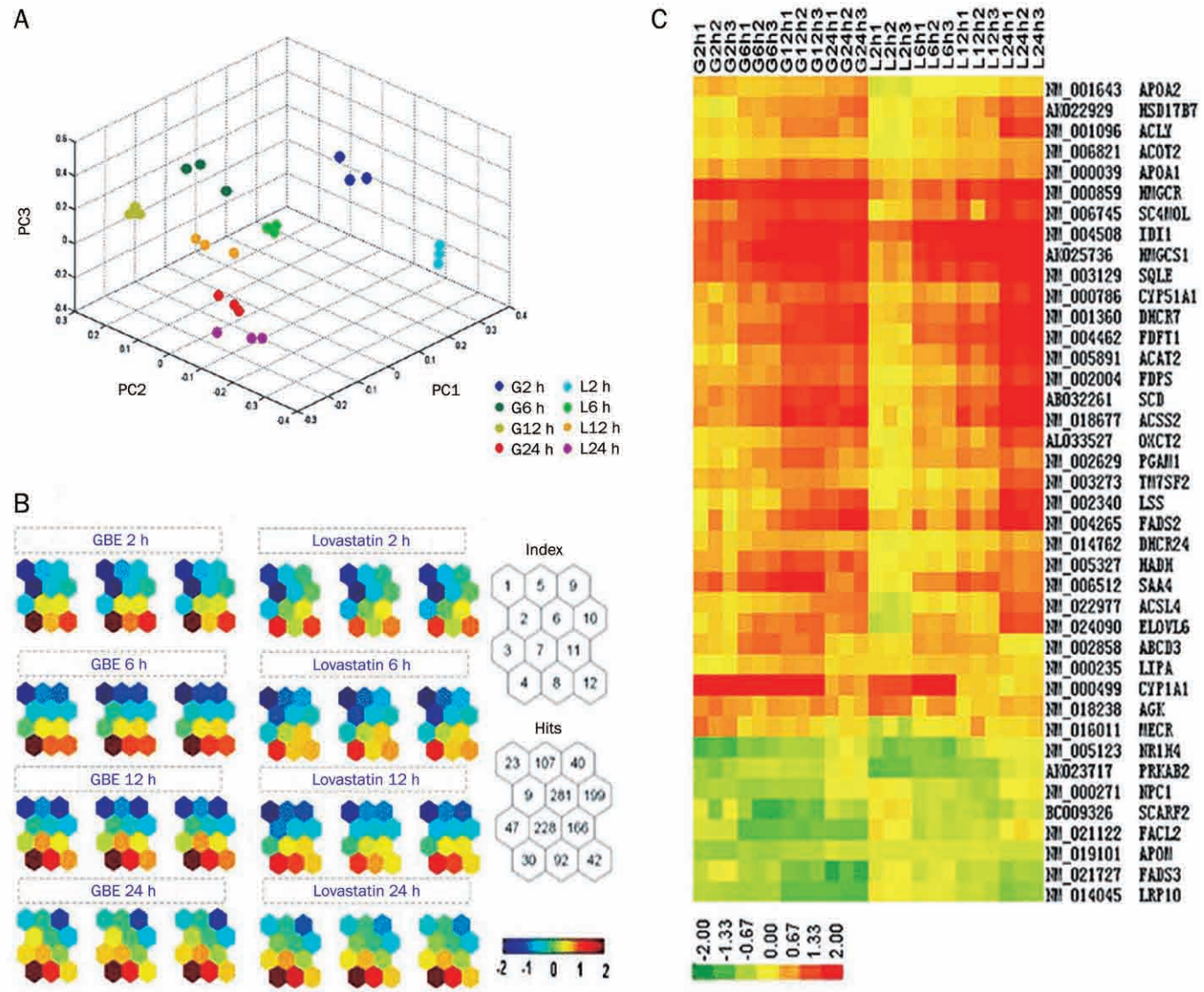

Figure 3. Dynamic changes in gene expression regulated by GBE and lovastatin. (A) Principal components analysis (PCA) of the filtered 9510 gene/ESTs from all samples. The PCA plot discriminated transcriptomic profiling of cells at different time points between GBE and lovastatin treatments. (B) Visualization of the SOM plots by CPP with the 1264 regulated genes/ESTs. Each presentation illustrates a sample specific transcription map, upregulated (red), downregulated (blue) and moderately regulated (yellow and green) genes were delineated. The color index stands for the log(2) transformed ratios. The triplicate samples were plotted individually to show the consistency of the biological replications. Index and number of genes contained in each section (hit) are indicated at the right. (C) Microarray analysis of the changes in lipid metabolism related genes that are regulated by GBE and lovastatin. Red represents upregulation, while green represents downregulation, and the color bar is indicated underneath. G represents GBE treatment, L represents lovastatin treatment.

assigned to groups based on their biological functions, such as lipid metabolism (Figure 3C), fibrinogenesis, trafficking, and metabolism (Figure S1). Detailed information on the regulated genes is provided in the supplementary material. Real-time RT-PCR was conducted on eight genes. *GAPDH* was used as an internal control because it was not modulated by GBE or lovastatin based on both the microarray and the semi-quantitative RT-PCR data (data not shown). The RT-PCR results demonstrated consistency with the microarray data (Figure S2).

We further distinguished the differential regulation between GBE and lovastatin treatment of 228 of the regulated genes/ESTs for at least one time point (Table S2). Of these 228 genes, a potential target of GBE and lovastatin could be identified and the different mechanisms of the two drugs could be derived. For example, the fibrinogen A gene (*FGA*) was significantly downregulated at an early time point with GBE, but not with lovastatin. Furthermore, *CYP1A1* was upregulated earlier and more strongly with GBE treatment compared with lovastatin treatment. In addition, *TGFBR3* was gradually upregulated by GBE but not regulated by lovastatin.

Regulation of the cholesterol metabolism pathway

Transcriptomic profiling revealed that GBE induced a significant change in the expression of genes in the cholesterol metabolic pathway. Genes involved in cholesterol biosynthesis, such as HMG-CoA reductase (*HMGCR*), isopentenyl-diphosphate delta isomerase 1 (*IDI1*), sterol *O*-acyltransferase (*SQLE*), HMG-CoA synthase 1 (*HMGCS1*), farnesyl-diphosphate farnesyltransferase 1 (*FDFT1*), farnesyl-diphosphate synthase (*FDPS*) and lanosterol synthase (*LSS*), were consistently upregulated (Figure 3C and Figure S3). *NR1H4*, which encodes the transcription factor farnesoid X receptor (*FXR*), was downregulated by both GBE and lovastatin. Additionally, transcriptomic profiling revealed that GBE downregulates genes associated with cholesterol uptake, including scavenger receptor class F member 2 (*SCARF2*), Niemann-Pick type C1 (*NPC1*) and LDL receptor-related protein 10 (*LRP10*) (Figure 3C).

We further examined 20 cholesterol metabolism-related genes by real-time RT-PCR. We identified that the mRNA levels of *HMGCR* and *SREBF2* (encoding sterol regulatory element-binding protein 2) were upregulated by GBE. On the other hand, the mRNA level of the *SREBF* chaperone (SCAP)

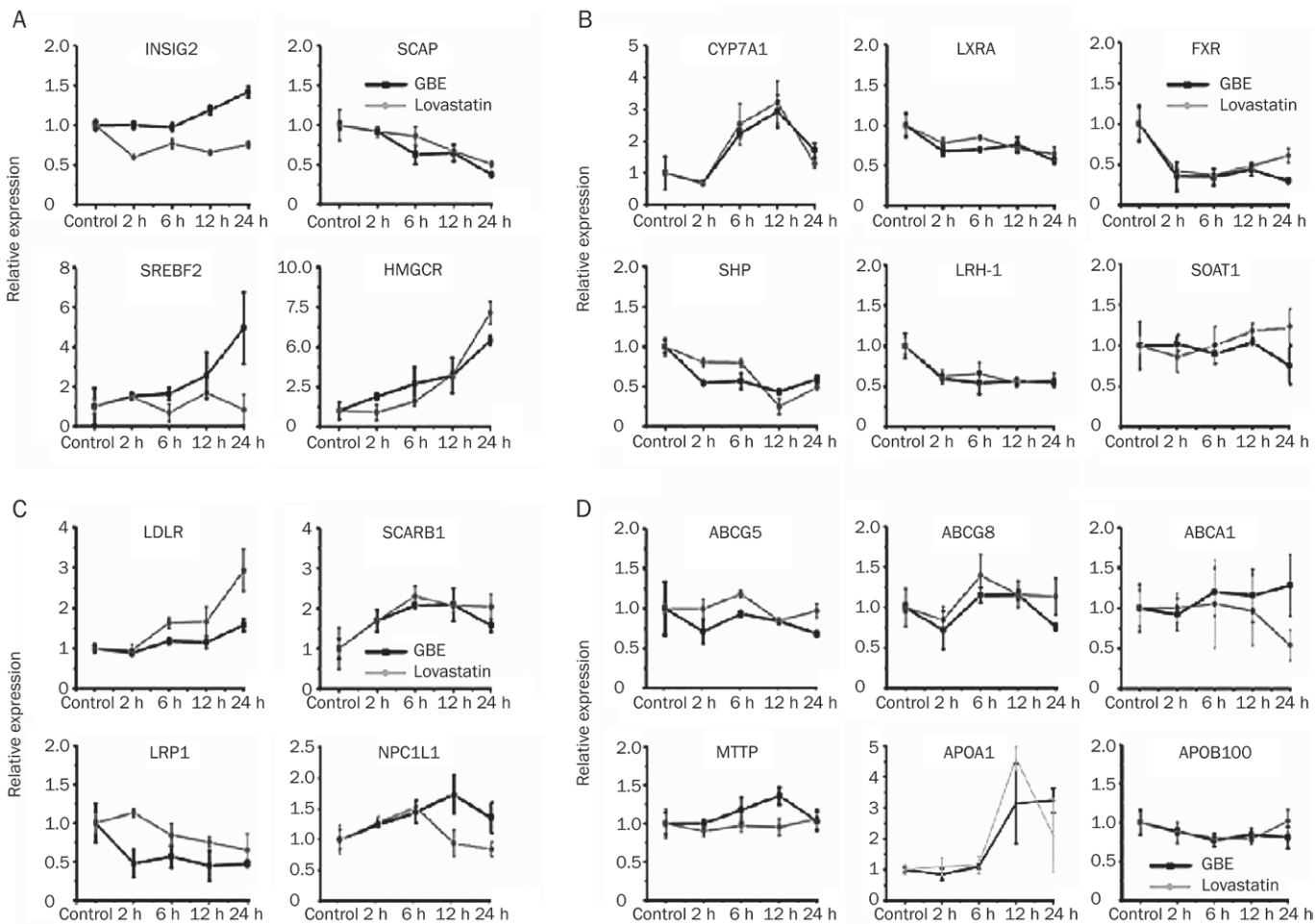

Figure 4. Examination of the cholesterol metabolism related genes with real-time PCR. *GAPDH* was used as an internal control. Gene expression was calculated with threshold cycles, the expression of each gene in the control group was set to 1. n=3. Data are presented as the relative average±SD.

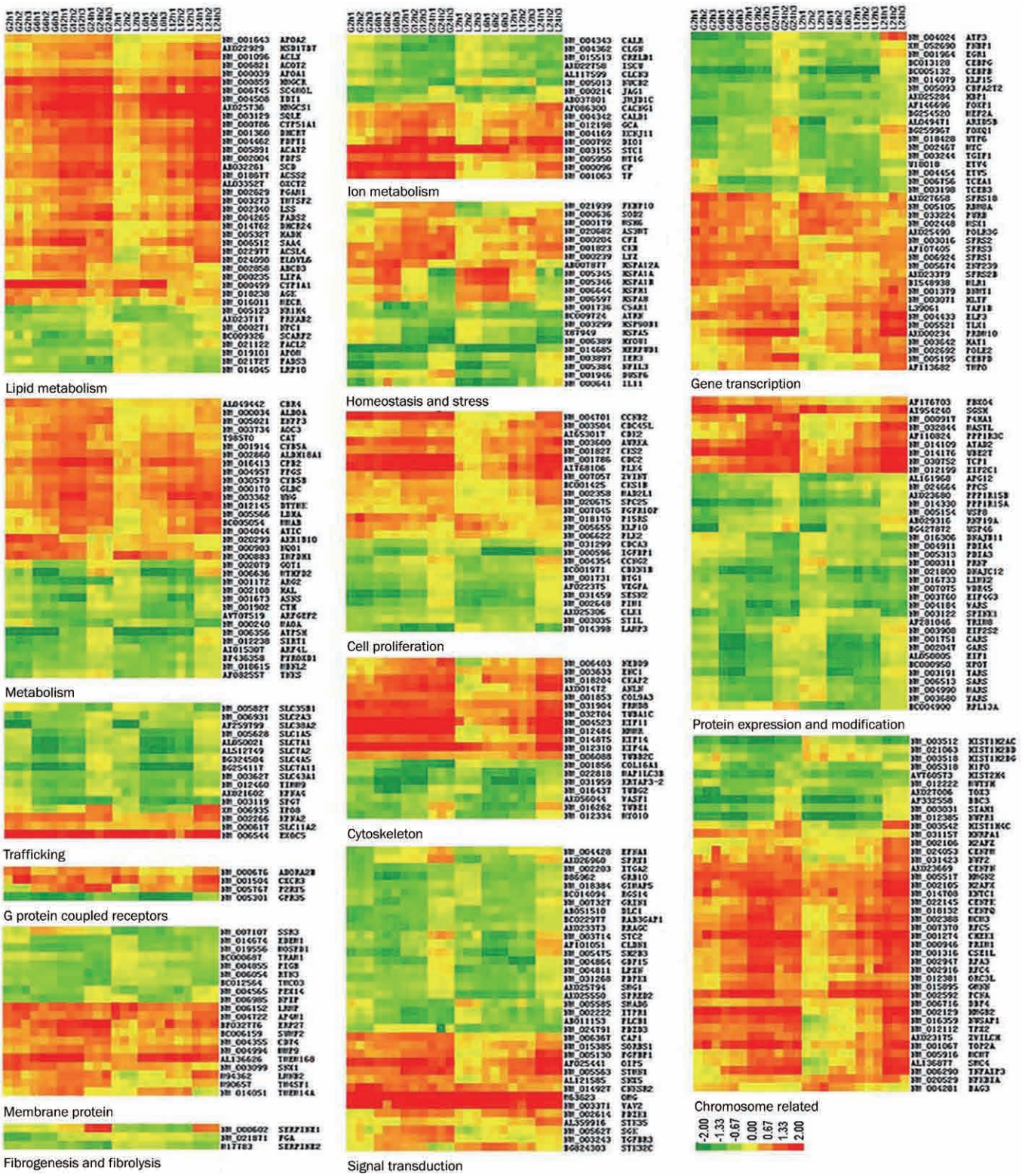

Figure S1. Functional categories of the representative genes that were regulated by GBE50 and lovastatin in HepG2 cells. Functional features of each gene were determined based on its ontology annotation and published literature. All the relevant genes are grouped by hierarchical clustering based on the expression regulation (log2ratios) across all the samples (www.shbiochip.com/research/GBE/HepG2). Log2 ratios were color coded as indicated.

was downregulated by GBE (Figure 4A). The protein level of both *HMGCR* and *SREBF2* encoding protein SREBP2 was also increased (Figure 5). Interestingly, insulin-induced gene 2 (*INSIG2*) was upregulated by GBE, but downregulated by

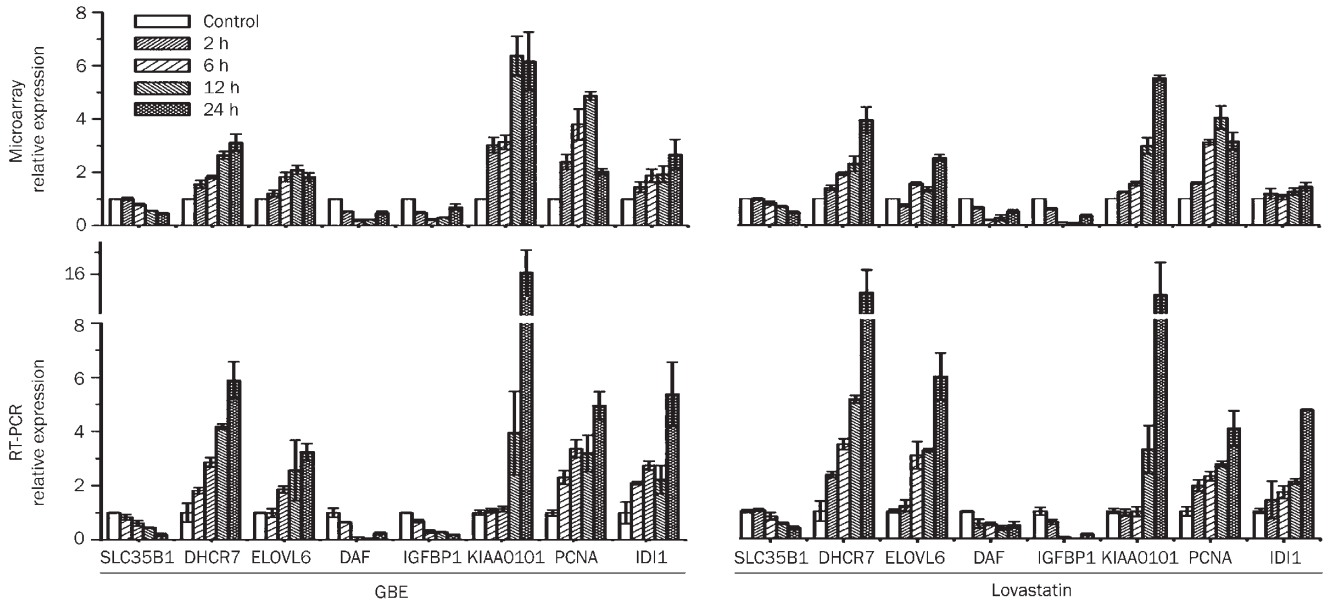

Figure S2. Validation of the microarray data with real-time RT-PCR for eight of the regulated genes. The results demonstrated a high concordance between the two methods.

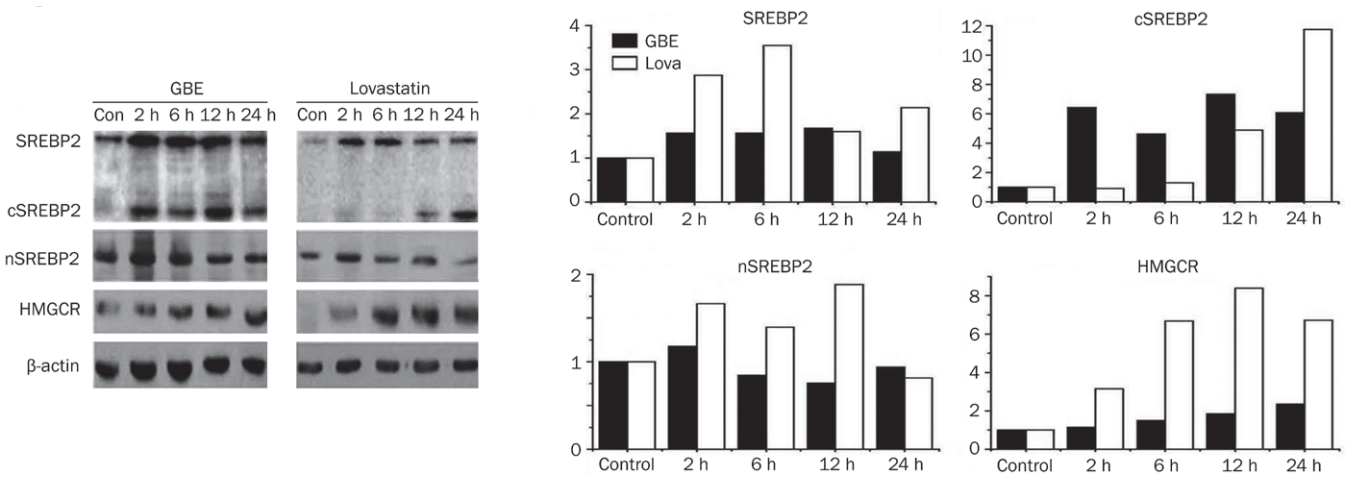

Figure 5. Western blot analysis of HMGCR and SREBP2 proteins. (A) Western blots images, (B) Signal quantitation of each band. β-actin was immunoprobed as a loading control. HMGCR was induced by both GBE50 and lovastatin, but the lovastatin had a stronger effect. The SREBP2 c-terminus was induced by GBE50 and lovastatin. The cleaved form of n-terminus nSREBP2 was upregulated by lovastatin, but not GBE50.

lovastatin.

GBE and lovastatin had similar regulatory effects on several genes involved in cholesterol catabolism. *CYP7A1* (encoding cholesterol 7-alpha-hydroxylase) was upregulated by treatment with both drugs. Genes encoding the transcription factors liver X receptor alpha (*LXRA*), farnesoid X receptor (*FXR*), orphan nuclear receptor (*SHP*), and liver receptor homolog 1 (*LRH-1*) were all downregulated by GBE and lovastatin. Sterol O-acyltransferase (*SOAT1*) was not significantly regulated by treatment with either GBE or lovastatin (Figure 4B).

Genes involved in cholesterol influx, such as the LDL receptor (*LDLR*), the scavenger receptor class B member 1 (*SCARB1*) and Niemann-Pick C1-like protein 1 (*NPC1L1*), were all upregulated by GBE and lovastatin. However, LDL-related protein 1 (*LRP1*) was downregulated. Lovastatin upregulated *LDLR*, but downregulated *LRP1* expression to a greater extent than GBE (Figure 4C). Cholesterol efflux-related genes, such as transporter genes, ATP-binding cassette 1 (*ABCA1*), ATP-binding cassette 5 (*ABCG5*), ATP-binding cassette 8 (*ABCG8*), microsomal triglyceride transfer protein (*MTTP*) and apolipoprotein B 100 (*APOB100*), were not significantly regulated. However, the cholesterol efflux gene apolipoprotein A–I (*APOA1*) was upregulated by both GBE and lovastatin (Figure 3D, Figure 6).

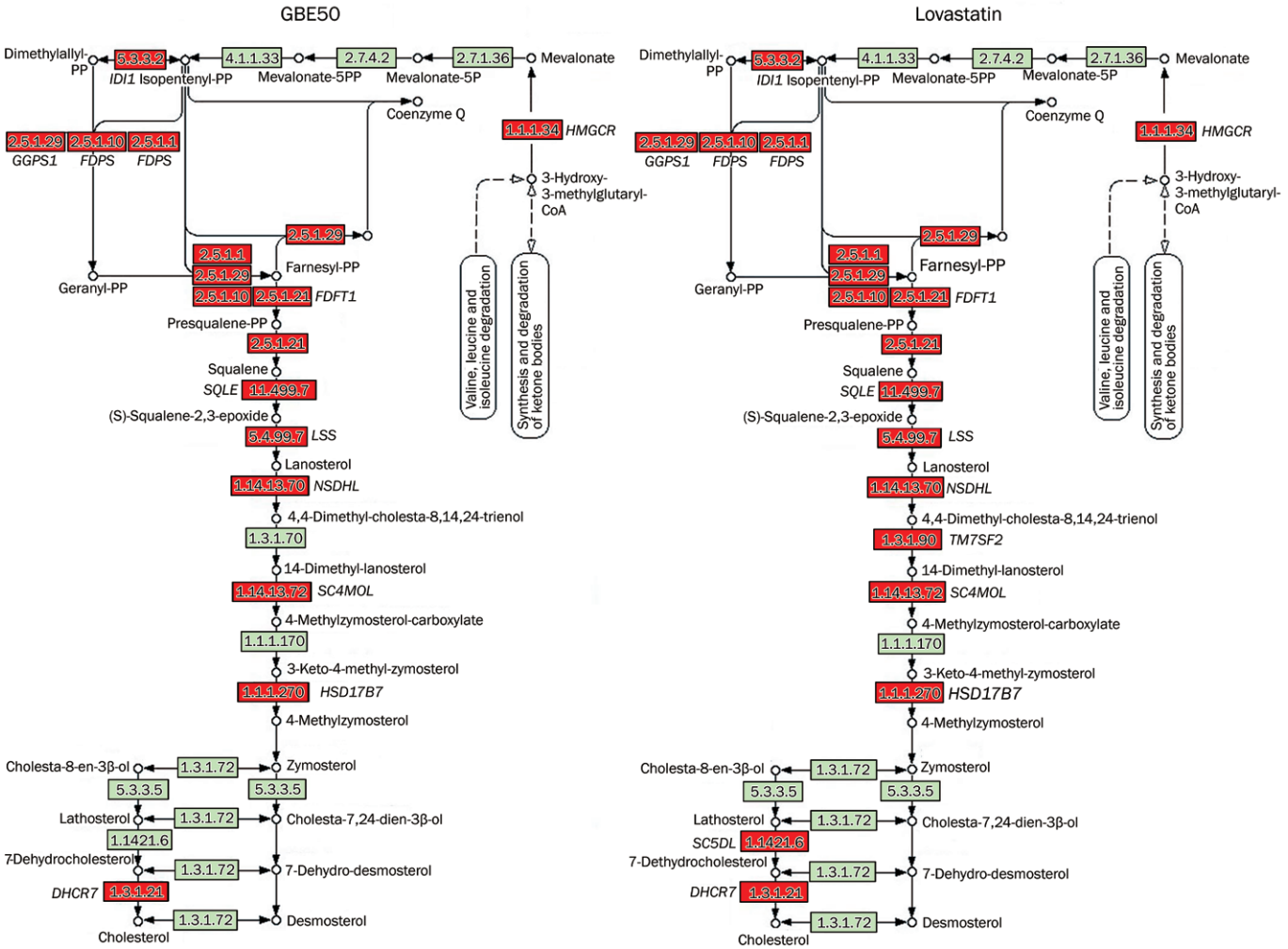

Figure S3. Genes involved in the cholesterol biosynthesis pathway were upregulated by GBE50 and/or lovastatin. Genes in red were observed to be over expressed, while the genes in light green indicate no significant changes.

Discussion

In the present study, the cholesterol lowering effect of GBE was demonstrated in cultured hepatocytes. We used lovastatin as a positive control because it functions as an HMG-CoA reductase inhibitor. Here, we demonstrate that GBE also inhibits the activity of HMG-CoA reductase in an *in vitro* enzymatic activity assay using hepatic microsomes. Based on the claim that flavonoids possess a blood cholesterol level-lowering effect by inhibiting HMG-CoA reductase activity[21] and the major component of GBE is flavonoids (~24%), it is likely that the flavonoids in GBE contribute to its cholesterol-lowering effect. However, the exact active components in GBE that are involved in lowering cellular cholesterol are not precisely known.

Based on the pleiotropic effects of GBE, we used transcriptomic profiling analysis to allow us to assess multiple genes simultaneously. We propose that this approach is essential for understanding the complex mechanisms of phytomedicines. Previous studies have widely used transcriptomic strategies to explore drug regulation networks[22, 23]. In the current study, transcriptomic profiling revealed that GBE induces significant gene expression changes in cultured hepatocytes. These data broadened our understanding of the molecular mechanisms by which GBE exerts its pleiotropic effects. In particular, our study focused on defining the molecular mechanisms by which GBE treatment modulates the genes involved in cholesterol metabolism.

Cholesterogenic genes are predominantly regulated through a feedback mechanism involving the cellular cholesterol pool. In this study, we show that GBE and lovastatin both lower cellular cholesterol by inducing an adaptive response in gene expression changes. Most members of the cholesterol biosynthesis pathway were increased. Additionally, we observed upregulation of *SREBF2*, a ubiquitously expressed transcription factor that controls cholesterol homeostasis by stimulating the transcription of sterol-regulated genes[24]. Thus, the observed upregulation of *SREBF2* and cholesterogenic genes suggests that GBE lowers cholesterol through an adaptive response. In addition *INSIG2*, an endoplasmic reticulum protein that binds *SCAP* and blocks the export of SREBPs to the

Table S2. List of genes with different regulations with GBE and lovastatin.

Genbank	Symbol	Genbank	Symbol	Genbank	Symbol	Genbank	Symbol
AI335447	ABCB6	BC008360	FAM113B	D29954	NCAPD3	AF113682	TMPO
NM_013375	ABT1	AB046794	FAM29A	NM_005381	NCL	NM_004237	TRIP13
NM_005891	ACAT2	NM_012300	FBXW11	BG612832	NEDD1	NM_015516	TSKU
NM_001096	ACLY	NM_004462	FDFT1	AB037925	NFKBIZ	NM_004615	TSPAN7
NM_001096	ACLY	R82935	FDPS	NM_000271	NPC1	NM_032704	TUBA1C
NM_022977	ACSL4	NM_002004	FDPS	NM_005013	NUCB2	NM_006088	TUBB2C
BC006121	AIFM2	NM_021871	FGA	NM_016359	NUSAP1	NM_014176	UBE2T
NM_020299	AKR1B10	NM_005130	FGFBP1	NM_002539	ODC1	NM_019116	UBFD1
NM_002860	ALDH18A1	NM_004497	FOXA3	AF025441	OIP5	NM_003362	UNG
AK026685	AMMECR1L	AF146696	FOXP1	NM_002568	PABPC1	NM_003368	USP1
NM_001145	ANG	NM_031904	FRMD8	NM_000919	PAM	AK023675	UTRN
U79297	ANKRD46	BC006997	G3BP1	NM_001618	PARP1	AK022888	WDFY1
AK001472	ANLN	NM_000512	GALNS	U80735	PAXIP1	NM_007086	WDHD1
NM_001153	ANXA4	NM_000821	GGCX	NM_002592	PCNA	D26488	WDR43
NM_001641	APEX1	NM_005271	GLUD1	NM_004911	PDIA4	BC002329	WIZ
NM_001643	APOA2	NM_006578	GNB5	BI761657	PIM3	NM_003400	XPO1
NM_001643	APOA2	NM_002106	H2AFZ	AI768106	PLK4	NM_021994	ZNF277P
NM_019101	APOM	NM_005327	HADH	NM_006903	PPA2	AF151023	ZNF581
NM_004044	ATIC	NM_003512	HIST1H2AC	NM_004703	RABEP1	AK023175	ZWILCH
NM_005504	BCAT1	NM_002129	HMGB2	NM_006479	RAD51AP1	NM_007057	ZWINT
AB067490	C14orf106	NM_000859	HMGCR	NM_002880	RAF1	AB012922	
NM_031210	C14orf156	XM_048933	HMGCS1	BC018163	RALB	AB032261	
NM_001735	C5	NM_005517	HMGN2	NM_007370	RFC5	AF076675	
BG216972	C6orf182	NM_012484	HMMR	NM_012249	RHOQ	AF196969	
AL133014	C7orf20	NM_020995	HPR	NM_024539	RNF128	AF305057	
AF086300	CACNG1	NM_003299	HSP90B1	NM_002947	RPA3	AF382013	
NM_004343	CALR	X87949	HSPA5	NM_005980	S100P	AI015307	
AL122079	CCDC14	NM_002157	HSPE1	NM_004757	SCYE1	AI128239	
NM_004701	CCNB2	NM_006389	HYOU1	NM_000602	SERPINE1	AI581732	
NM_004354	CCNG2	BC002640	IFT20	NM_003016	SFRS2	AK023379	
NM_001786	CDC2	NM_000883	IMPDH1	AF107405	SFRS3	AK025736	
NM_005195	CEBPD	NM_014869	IQSEC1	NM_000617	SLC11A2	AL035689	
NM_018132	CENPQ	AL049321	IRAK1BP1	NM_006841	SLC38A3	AL110194	
NM_000204	CFI	NM_033666	ITGB1	NM_003090	SNRPA1	AL137144	
BC001425	CKS1B	NM_002217	ITIH3	AL121585	SNX5	AV721426	
NM_001856	COL16A1	BG035179	KCTD11	NM_000454	SOD1	AV743808	
AK024070	CTPS2	AB006624	KIAA0286	NM_000636	SOD2	BC000222	
NM_001908	CTSB	AL390128	KIAA1530	NM_003105	SORL1	BC001209	
NM_030579	CYB5B	AB051499	KIAA1712	NM_003105	SORL1	BC013135	
NM_000499	CYP1A1	NM_014875	KIF14	NM_020675	SPC25	BF508697	
NM_018122	DARS2	NM_012310	KIF4A	NM_003122	SPINK1	BF570946	
NM_006716	DBF4	NM_002266	KPNA2	AK025550	SPRED2	D63874	
NM_014762	DHCR24	NM_002296	LBR	NM_003129	SQLE	D80000	
BC007339	DHRS2	NM_005566	LDHA	AL359916	STK35	NM_001101	
NM_016306	DNAJB11	NM_000235	LIPA	NM_003600	STK6	NM_001731	
U97105	DPYSL2	M94362	LMNB2	AF131808	STX7	NM_002950	
NM_012145	DTYMK	U28831	LOC400986	AF058954	SUCLG2	NM_004169	
NM_004428	EFNA1	NM_002358	MAD2L1	NM_030752	TCP1	NM_005899	
NM_012199	EIF2C1	NM_032844	MASTL	NM_003217	TEGT	NM_006821	
NM_003750	EIF3A	NM_002388	MCM3	NM_003243	TGFBR3	NM_007021	
NM_004433	ELF3	NM_002388	MCM3	NM_005521	TLX1	NM_007363	
NM_003633	ENC1	NM_016011	MECR	M90657	TM4SF1	NM_012112	
NM_014805	EPM2AIP1	NM_004994	MMP9	NM_003963	TM4SF5	NM_016126	
NM_001981	EPS15	NM_005591	MRE11A	NM_003273	TM7SF2	NM_031157	
NM_001982	ERBB3	NM_000251	MSH2	AL136626	TMEM168	R89610	
AF086028	ERBB3	NM_002455	MTX1	NM_004872	TMEM59	T49106	
AL512760	FADS1	NM_014865	NCAPD2	L19183	TMEM97	XM_051499	

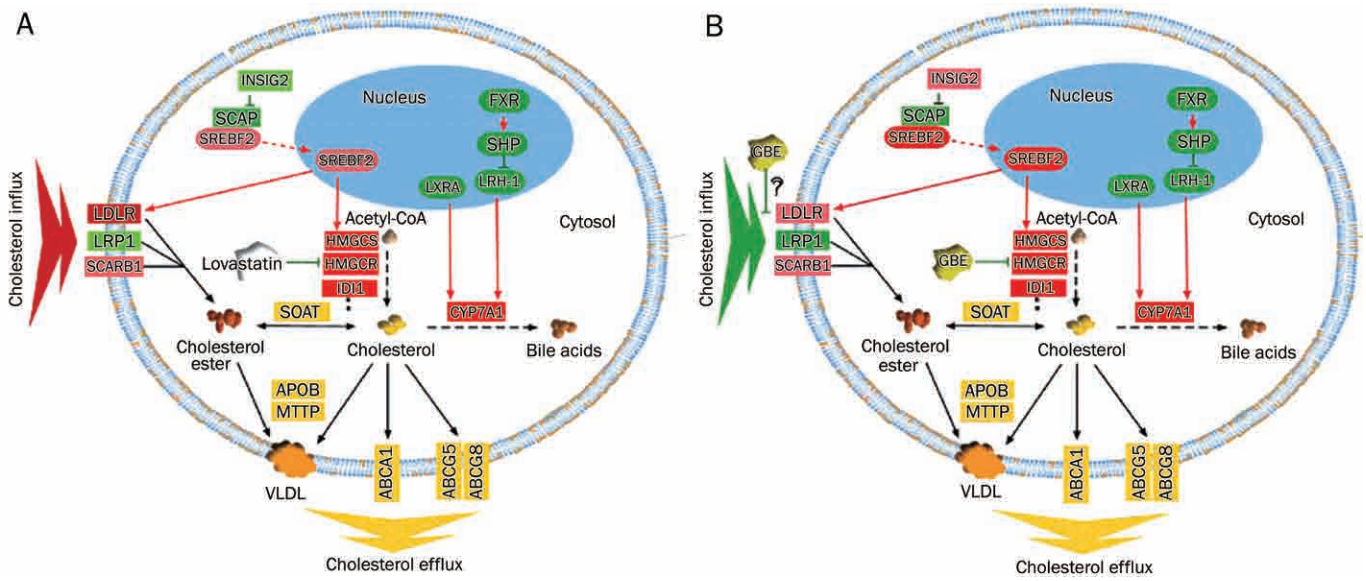

Figure 6. Ideogram illustration of the gene regulation networks underlying the cholesterol-lowering effect of GBE and lovastatin treatment in HepG2 cells. (A) GBE treatment. (B) Lovastatin treatment. The genes in green were down-regulated, while the genes in red were over-expressed, the yellow color represents genes that were not significantly changed, the red arrows indicated stimulation, the green line with block represents negative regulation. The following theme is proposed: lovastatin lowers cellular cholesterol content by inhibiting *de novo* biosynthesis by modulating the expression of the rate limiting enzyme, HMGCR, and inducing adaptive responses, such as the over expression of genes involved in cholesterol endogenous biosynthesis and cholesterol influx, and the down-regulation of genes related to cholesterol catabolism into bile acids, which are required for the maintenance of the homeostasis of cellular cholesterol. With respect to molecular mechanisms downstream of GBE treatment, in addition to inhibiting HMGCR, cholesterol influx was also inhibited and related gene expression changes were demonstrated.

Golgi[25], was differentially regulated by GBE and lovastatin. These data suggest that GBE and lovastatin possess differential mechanisms for lowering cholesterol.

Cholesterol 7-alpha-hydroxylase (*CYP7A1*) is the rate-limiting enzyme that converts cholesterol to bile acids. The oxysterol receptor, liver X receptor alpha (*LXRA*), is the dominant regulator of *CYP7A1* transcription[26]. The bile acid receptor, *FXR*, is activated by bile acids and subsequently represses *CYP7A1* expression through a regulatory cascade involving SHP and LRH-1[27]. In this study, *LXRA*, *FXR*, *SHP*, and *LRH-1* were consistently downregulated by both GBE and lovastatin. Interestingly, *CYP7A1* was upregulated by both cholesterol-lowering agents. Although *CYP7A1* was upregulated, we propose that the catabolism of cholesterol to bile acids might be diminished because both the bile acid biosensor, *FXR*, and the dominant regulator were downregulated.

As a feedback response to the cellular cholesterol-lowering effects, lovastatin induced the overexpression of *LDLR* and *SCARBI*. *LDLR*, the LDL receptor, is involved in receptor-mediated endocytosis of LDL and is regulated by *SREBP2*[28]. *SCARBI* (Scavenger receptor class B type I) is a high-density lipoprotein (HDL) receptor in the liver and is involved in the selective uptake of cholesteryl ester from HDL that is involved in the reverse cholesterol transport (RCT)[29]. Thus, the overexpression of *LDLR* and *SCARBI* could facilitate cholesterol uptake from the medium to maintain the homeostasis of the cellular cholesterol pool. However, we found that GBE inhibits the uptake of cholesterol from the medium. This result is consistent with a previous study by Qiu *et al*, in which GBE inhibited the hyperpermeability of endothelial cells to [^{125}I]-labeled oxLDL[30]. The mild upregulation of *LDLR* and the strong downregulation of *LRP1* and *LRP10* indicate that GBE is a cholesterol uptake inhibitor, although the exact mechanisms by which GBE inhibits cholesterol uptake were not identified.

The liver is largely responsible for maintaining cholesterol homeostasis. In the present study, we find that GBE inhibits cholesterol influx in HepG2 cells. These data imply that cholesterol clearance from the blood into the liver might be restrained. Although the cellular global HMG-CoA reductase activity in cells was not pursued in this study, the *in vitro* inhibition of HMG-CoA reductase activity suggests an attenuation of endogenous cholesterol biosynthesis. This was in agreement with our previous findings that GBE mildly inhibits the elevation of blood cholesterol levels and liver lipid accumulation induced by high-fat diet in rats[31].

In conclusion, both GBE and lovastatin lowered the cholesterol content in cultured hepatocytes. GBE exhibited dual effects on both HMG-CoA reductase activity and cholesterol influx inhibition. The proposed similar and unique mechanisms of cholesterol lowering by GBE and lovastatin are summarized in Figure 6. Further investigation of the genes regulated by GBE is of particular importance both for understanding the unique mechanisms by which GBE regulates cholesterol metabolism and for the clinical application of GBE.

Supplementary material

Transcriptome regulations with GBE50 and lovastatin in HepG2 cells

Among the regulated genes with ontology annotations, 254 were assigned into groups based on their biological functions (Figure S1).

Lipid metabolism pathways were affected by both drugs

Most members of the cholesterol biosynthesis pathway were upregulated in both treatment groups, including the rate limiting enzyme, 3-hydroxy-3-methylglutaryl-coenzyme A reductase (*HMGCR*), isopentenyl-diphosphate delta isomerase 1 (*IDIl*), squalene epoxidase (*SQLE*), 3-hydroxy-3-methylglutaryl-coenzyme A synthase 1 (*HMGCS1*), farnesyl-diphosphate farnesyltransferase 1 (*FDFT1*), farnesyl-diphosphate synthase (*FDPS*), lanosterol synthase (*LSS*), *etc*. Genes involved in cholesterol uptake, such as the scavenger receptor class F member (*SCARF2*) and Niemann-Pick disease-type C1 (*NPC1*) were downregulated in both treatment groups. The cellular cholesterol content sensing transcription factor, farnesoid X receptor (FXR) (*NR1H4*), was observed to be down regulated. The genes encoding the fatty acid metabolism enzymes were also significantly regulated. Acyl-CoA synthetase (*ACSS2*), stearoyl-CoA desaturase (*SCD*), hydroxyacyl-coenzyme A dehydrogenase (HADH), fatty acid desaturase 2 (*FADS2*) and 3-oxoacid CoA transferase 2 (*OXCT2*) were upregulated in both treatment groups. However, fatty-acid-coenzyme A ligase (*FACL2*), fatty acid desaturase 3 (*FADS3*), as well as low density lipoprotein receptor-related protein 10 (*LRP10*), were more strongly downregulated by GBE50 than lovastatin.

Regulations of transporters with two drugs

Downregulation of the solute carrier proteins (*SLC1A5*, *SLC2A3*, *SLC4A5*, *SLC7A1*, *SLC7A2*, *SLC7A11*, *SLC35B1*, *SLC38A2*, *SLC43A1*), and the translocase of inner mitochondrial membrane 9 (*TIMM9*) revealed that cellular substance intracellular trafficking was inhibited by the both drugs. Additionally, our microarray analysis revealed that the exocyst complex component 5 (*EXOC5*), which is essential for post-Golgi traffic, was upregulated.

Regulation of energy metabolism related genes

The acute repression of mitochondrial H^+ transporting ATP synthase subunit (*ATP5H*) was detected as early response to the treatment with both GBE and lovastatin; however, the expression levels were recovered to a normal level when treated for 24 h, suggesting that energy metabolism was inhibited at an early stage when treated with either drug, but the effect only lasted for a short period. Similarly, carbohydrate metabolism-associated genes, including lactate dehydrogenase A (*LDHA*), aldehyde dehydrogenase member (*ALDH18A1*), nucleic acid metabolism related uracil-DNA glycosylase (*UNG*), inosine monophosphate dehydrogenase (*IMPDH1*), *etc*, were upregulated. Downregulation of glutamic-oxaloacetic transaminase (*GOT1*), methylenetetrahydrofolate dehydrogenase 2 (*MTHFD2*), arginase (*AARG2*) suggested that these drugs also inhibited amino acid metabolism. The downregulation of monoamine oxidase A (*MAOA*) is associated with a neurotransmitter degradation reduction. The early upregulation of carbonyl reductase 4 (*CBR4*), aldolase A (*ALDOA*), aldose reductase (*AKR1B10*) and vascular adhesion protein 1 (amine oxidase, copper containing 3) (*AOC3*) by only GBE50 suggests that these genes are not regulated by lovastatin.

Cell signaling and communication gene expression regulations

The expression of cell-cell communication and signaling genes, including oligodendrocyte myelin glycoprotein (*OMG*) and Vav 2 oncogene (*VAV2*), were upregulated by both drugs at an early time point and the effects lasted at least 24 h. Serum/glucocorticoid regulated kinase (*SGK*) and transforming growth factor, beta receptor III (*TGFBR3*), fibroblast growth factor binding protein 1 (*FGFBP1*), and adenylate cyclase-associated protein 1 (*CAP1*) were upregulated with GBE50 treatment, but were either not regulated or regulated at a late time point by lovastatin treatment. Expression of the PDZ domain containing protein coding gene (*PDZD3*) was down regulated at earliest time point in both treatment groups, and was observed to rapidly recover to normal levels in the GBE50 treatment group, but remained repressed with lovastatin treatment. It is important to point out that the iron metabolism members, ceruloplasmin (ferroxidase) (*CP*) and transferrin (*TF*), were both rapidly upregulated by GBE50, but only slightly regulated at 24 h with lovastatin, and the downregulation of a calcium binding protein, nucleobindin 2 (*NUCB2*), occurred later with lovastatin than with GBE.

Protein translation and modification members

The stress response heat shock proteins (*HSPA1A*, *-A8*, *-H1*) were upregulated with lovastatin treatment earlier than with GBE50, and FK506 binding protein 10 (*FKBP10*) and dual specificity phosphatase 6 (*DUSP6*) were both downregulated by lovastatin at the earliest time point, but are neither up- nor downregulated by GBE50 treatment. The finding that the plasminogen activator inhibitor member 1 (*SERPINE1*) was upregulated, the member 2 (*SERPINE2*) was down regulated in both groups, and fibrinogen A (*FGA*) was repressed by GBE50, but not lovastatin at the early time point, all indicate that fibrinolysis is regulated by these two drugs.

General transcription regulators

Regulation of most transcription and protein expression/modification factors were similar between the two groups, except for the zinc finger protein (*ZNF239*), F-box protein 4 (*FBXO4*), proline 4-hydroxylase (*P4HA1*) and a member of the ubiquitin-conjugating enzyme (*UBE2T*), which were upregulated, and a serine peptidase inhibitor (*SPINK1*), which was downregulated earlier in the GBE50 treatment group, and the ribosomal protein L13a (*RPL13A*) was repressed in the lovastatin group only.

Chromosome structure protein genes

Chromosome histone coding genes were downregulated in both groups. *HIST1H2AC*, *HIST1H2BD*, *HIST1H2BG* were downregulated earlier in the GBE50 group than with lovastatin. High-mobility group box 2 (*HMGB2*), nucleolar and spindle associated protein (*NUSAP1*), microtubule-associated protein (*TPX2*), kinetochore associated protein (*ZWILCH*), topoisomerase (*TOP2*) and tumor necrosis factor alpha-induced protein 3 (*TNFAIP3*) were all upregulated earlier, while ribonucleoprotein A1 (*HNRPA1*) was upregulated only with GBE50, compared to lovastatin.

Membrane proteins

The signal sequence receptor gamma (*SSR3*) was down-

regulated with lovastatin at an early time point, while GBE50 had no effect on its regulation. Transmembrane 4 superfamily member 1 (*TM4SF1*) and lamin B2 (*LMNB2*) were upregulated with GBE50 earlier than lovastatin, whereas *MOSPD1*, *PIGB*, *RTN3*, and *TMCO3* had earlier repression with GBE50 treatment than with lovastatin.

Cell proliferation members

Cell proliferation was enhanced with GBE50 compared to lovastatin. Cell proliferation promoting genes, including *CCNB2*, *CDC2*, *AURKA*, *PLK4*, *MAD2L1*, were upregulated earlier with GBE50 treatment than with lovastatin. This result was also observed in the cell division or motility related cytoskeleton protein coding genes, *eg*, *CKAP2*, *ANLN*, *KIF11*, *-14*, *HMMR*, *TUBA1C*, *FRMD8*. However, *LAMP3*, *TUBG2,* and *COL16A1* demonstrated earlier repression in the GBE treatment group.

Acknowledgments

This work was financially supported by grants from the Chinese National High Tech Program (863-2003AA2032) and the Development Projects of Shanghai Commission of Science and Technology (03DZ19551, 05DZ19738, 06DZ19727).

We thank Hua-sheng XIAO, Zhi-dong ZHU, Jun-song HAN, Kai SONG, and Huai-guang SONG of the SBC for their technical support and constructive comments. We also thank Dr Qing ZHANG of Shanghai Institute of Plant Physiology and Ecology for help with liquid scintillation measurements. We thank Qi GAO and Guo-an ZHANG of Shanghai Xingling Pharmaceutical Co for providing the *Ginkgo biloba* extract products and their support.

Author contribution

Zuo-quan XIE and Lu ZHANG designed and conducted biochemistry measurements, RT-PCR, Western blot, and data exploration; Sai YE cultured the cells; Yi QU, Qi WANG, Yang GAO, and Ji ZHANG analyzed the data; Li-bo LIN performed the microarray experiment; Gai LIANG and Hui WANG performed the HMG-CoA reductase activity assays; Guo-ping ZHAO commented on experimental data; Qing-hua ZHANG designed the experiments, examined the data and wrote the manuscript.

References

1 Sharpless KE, Thomas JB, Christopher SJ, Greenberg RR, Sander LC, Schantz MM, *et al*. Standard reference materials for foods and dietary supplements. Anal Bioanal Chem 2007; 389: 171–8.

2 Ramassamy C, Longpre F, Christen Y. *Ginkgo biloba* extract (EGb 761) in Alzheimer's disease: is there any evidence? Curr Alzheimer Res 2007; 4: 253–62.

3 Luo Y, Smith JV, Paramasivam V, Burdick A, Curry KJ, Buford JP, *et al*. Inhibition of amyloid-beta aggregation and caspase-3 activation by the *Ginkgo biloba* extract EGb761. Proc Natl Acad Sci USA 2002; 99: 12197–202.

4 Bridi R, Crossetti FP, Steffen VM, Henriques AT. The antioxidant activity of standardized extract of *Ginkgo biloba* (EGb 761) in rats. Phytother Res 2001; 15: 449–51.

5 Liu CS, Cheng Y, Hu JF, Zhang W, Chen NH, Zhang JT. Comparison of antioxidant activities between salvianolic acid B and *Ginkgo biloba* extract (EGb 761). Acta pharmacol Sin 2006; 27: 1137–45.

6 Wu ZM, Yin XX, Ji L, Gao YY, Pan YM, Lu Q, *et al*. *Ginkgo biloba* extract prevents against apoptosis induced by high glucose in human lens epithelial cells. Acta Pharmacol Sin 2008; 29: 1042–50.

7 Mahady GB. *Ginkgo biloba* for the prevention and treatment of cardiovascular disease: a review of the literature. J Cardiovasc Nurs 2002; 16: 21–32.

8 Cho HJ, Nam KS. Inhibitory effect of ginkgolide B on platelet aggregation in a cAMP- and cGMP-dependent manner by activated MMP-9. J Biochem Mol Biol 2007; 40: 678–83.

9 Kudolo GB, Wang W, Barrientos J, Elrod R, Blodgett J. The ingestion of *Ginkgo biloba* extract (EGb 761) inhibits arachidonic acid-mediated platelet aggregation and thromboxane B2 production in healthy volunteers. J Herb Pharmacother 2004; 4: 13–26.

10 Yao ZX, Han Z, Drieu K, Papadopoulos V. *Ginkgo biloba* extract (Egb 761) inhibits beta-amyloid production by lowering free cholesterol levels. J Nutr Biochem 2004; 15: 749–56.

11 Igarashi K, Ohmuma M. Effects of isorhamnetin, rhamnetin, and quercetin on the concentrations of cholesterol and lipoperoxide in the serum and liver and on the blood and liver antioxidative enzyme activities of rats. Biosci Biotechnol Biochem 1995; 59: 595–601.

12 Lin SJ, Yang TH, Chen YH, Chen JW, Kwok CF, Shiao MS, *et al*. Effects of *Ginkgo biloba* extract on the proliferation of vascular smooth muscle cells *in vitro* and on intimal thickening and interleukin-1beta expression after balloon injury in cholesterol-fed rabbits *in vivo*. J Cell Biochem 2002; 85: 572–82.

13 Rodriguez M, Ringstad L, Schafer P, Just S, Hofer HW, Malmsten M, *et al*. Reduction of atherosclerotic nanoplaque formation and size by *Ginkgo biloba* (EGb 761) in cardiovascular high-risk patients. Atherosclerosis 2007; 192: 438–44.

14 Huang TH, Peng G, Li GQ, Yamahara J, Roufogalis BD, Li Y. Salacia oblonga root improves postprandial hyperlipidemia and hepatic steatosis in Zucker diabetic fatty rats: activation of PPAR-alpha. Toxicol Appl Pharmacol 2006; 210: 225–35.

15 Philipp BW, Shapiro DJ. Improved methods for the assay and activation of 3-hydroxy-3-methylglutaryl coenzyme A reductase. J Lipid Res 1979; 20: 588–93.

16 Huang J, Sheng HH, Shen T, Hu YJ, Xiao HS, Zhang Q, *et al*. Correlation between genomic DNA copy number alterations and transcriptional expression in hepatitis B virus-associated hepatocellular carcinoma. FEBS Lett 2006; 580: 3571–81.

17 Li RY, Zhang QH, Liu Z, Qiao J, Zhao SX, Shao L, *et al*. Effect of short-term and long-term fasting on transcriptional regulation of metabolic genes in rat tissues. Biochem Biophys Res Commun 2006; 344: 562–70.

18 Yang YH, Dudoit S, Luu P, Lin DM, Peng V, Ngai J, *et al*. Normalization for cDNA microarray data: a robust composite method addressing single and multiple slide systematic variation. Nucleic Acids Res 2002; 30: e15.

19 Tusher VG, Tibshirani R, Chu G. Significance analysis of microarrays applied to the ionizing radiation response. Proc Natl Acad Sci USA 2001; 98: 5116–21.

20 Zheng PZ, Wang KK, Zhang QY, Huang QH, Du YZ, Zhang QH, *et al*. Systems analysis of transcriptome and proteome in retinoic acid/arsenic trioxide-induced cell differentiation/apoptosis of promyelocytic leukemia. Proc Natl Acad Sci U S A 2005; 102: 7653–8.

21 Havsteen BH. The biochemistry and medical significance of the flavonoids. Pharmacol Ther 2002; 96: 67–202.

22 Du Y, Wang K, Fang H, Li J, Xiao D, Zheng P, *et al*. Coordination of intrinsic, extrinsic, and endoplasmic reticulum-mediated apoptosis by imatinib mesylate combined with arsenic trioxide in chronic myeloid

leukemia. Blood 2006; 107: 1582–90.
23 Watanabe CM, Wolffram S, Ader P, Rimbach G, Packer L, Maguire JJ, *et al*. The *in vivo* neuromodulatory effects of the herbal medicine *Ginkgo biloba*. Proc Natl Acad Sci USA 2001; 98: 6577–80.
24 Eberle D, Hegarty B, Bossard P, Ferre P, Foufelle F. SREBP transcription factors: master regulators of lipid homeostasis. Biochimie 2004; 86: 839–48.
25 Yabe D, Brown MS, Goldstein JL. Insig-2, a second endoplasmic reticulum protein that binds SCAP and blocks export of sterol regulatory element-binding proteins. Proc Natl Acad Sci USA 2002; 99: 12753–8.
26 Wang J, Einarsson C, Murphy C, Parini P, Bjorkhem I, Gafvels M, *et al*. Studies on LXR- and FXR-mediated effects on cholesterol homeostasis in normal and cholic acid-depleted mice. J Lipid Res 2006; 47: 421–30.
27 Goodwin B, Jones SA, Price RR, Watson MA, McKee DD, Moore LB, *et al*. A regulatory cascade of the nuclear receptors FXR, SHP-1, and LRH-1 represses bile acid biosynthesis. Mol Cell 2000; 6: 517–26.
28 Horton JD, Shah NA, Warrington JA, Anderson NN, Park SW, Brown MS, *et al*. Combined analysis of oligonucleotide microarray data from transgenic and knockout mice identifies direct SREBP target genes. Proc Natl Acad Sci USA 2003; 100: 12027–32.
29 Connelly MA, Williams DL. Scavenger receptor BI: a scavenger receptor with a mission to transport high density lipoprotein lipids. Curr Opin Lipidol 2004; 15: 287–95.
30 Qiu Y, Rui YC, Li TJ, Zhang L, Yao PY. Inhibitory effect of extracts of *Ginkgo biloba* leaves on VEGF-induced hyperpermeability of bovine coronary endothelial cells *in vitro*. Acta Pharmacol Sin 2004; 25: 1306–11.
31 Gu X, Xie Z, Wang Q, Liu G, Qu Y, Zhang L, *et al*. Transcriptome profiling analysis reveals multiple modulatory effects of *Ginkgo biloba* extract in the liver of rats on a high-fat diet. Febs J 2009; 276: 1450–8.